Green preparation and evaluation of anti-psoriatic activity of vesicular elastic nanocarriers of kojic acid from *Aspergillus oryzae N12*; repurposing of dermo-cosmetic lead

Ashaimaa Y. Moussa (ashaimaa_yehia@pharma.asu.edu.eg)
Ain-Shams University
Haidy Abbas
Damanhour University
Mariam Zewail
Damanhour University
Passent M.E. Gaafar
Arab Academy for Science, Technology and Maritime Transport
Nehal Ibrahim
Ain-Shams University

Article

Keywords: Kojic acid, Aspergillus oryzae, psoriasis, spanlastics, docking, endophytes

Posted Date: December 12th, 2023

DOI: https://doi.org/10.21203/rs.3.rs-3738811/v1

Additional Declarations: No competing interests reported.

Abstract

Psoriasis is a skin disorder characterized by impaired epidermal differentiation that is regularly treated by many systemic drugs with numerous side effects. Our present work aims to investigate an efficient topical bio-friendly vesicular system loaded with kojic acid as an alternative way for the management of psoriasis to avoid systemic toxicity. To achieve our goal, kojic acid was isolated from the endophytic fungus *Aspergillus oryzae* N12 obtained from the stems of *Tecomaria capensis* (Bignoniaceae). Kojic acid-loaded spanlastics were prepared by ethanol injection technique; employing span 60 along with birj35 and cremophor rh40 as edge activators with the complete *in vitro* characterization of kojic acid-loaded spanlastics. The optimal formulation displayed spherical morphology under transmission electron microscopy, optimum particle size of 234.2 ± 1.65 nm and high entrapment efficiency (87.4 ± 0.84%). The selected formulation demonstrated significant sustained drug release compared with the drug solution. Kojic acid-loaded spanlastics demonstrated superior relief of psoriasis symptoms and the ability to maintain healthy skin with the least changes in mRNA expression of inflammatory cytokines compared to kojic solution *in vivo* studies. Moreover, *in vivo*, histopathological studies confirmed the safety of topically applied spanlastics. Concisely, our results suggest that a topically applied vesicular system loaded with kojic acid could lead to expansion in the dermo-cosmetic use of kojic acid as a natural bio-friendly alternative for occasionally used systemic anti-psoriatic drugs.

1. Introduction

Fungal metabolites are more than ever before becoming the source of bioactive compounds of diverse bioactivities [1, 2]. The genetic flexibility conferred by fungi and the fact that various cultures of the same strain can yield various chemical profiles, what is known as OMICS, prepared fungal endophytes to be the richest natural products repository [3]. The last decades have witnessed a growing impetus in fungal endophytes as bountiful microbial factories of secondary metabolites for various biotechnological applications on medicinal, agricultural and industrial levels [4]. Genus *Aspergillus* constitutes one of the tremendous fungal reservoirs of bioactive compounds with impressively immense chemical diversity and enriched biological repertoire [5]. Among the identified 378 *Aspergillus* species, *A. oryzae* represents one of the most dominant fungal species [6]. *A. flavus* was reported to be the most efficient hyper-producing strain of kojic acid (Fig. 1) [7]. The latter is among the prevalent chemical entities in the dermo-cosmetic industry because of its potent skin-whitening properties. By chelating two Cu^{2+} ions in the tyrosinase enzyme active site, kojic acid inhibits melanin synthesis leading to depigmentation. In addition, this pyranone has a plethora of applications in the food industry, dental care products and the pharmaceutical sector due to its anti-browning, bleaching, antioxidant, anti-inflammatory, antidiabetic, anticancer, antimicrobial, and antiparasitic properties [7]. Because of its diverse spectrum of applications, the kojic acid market has been on the rise and it is anticipated that by 2026, the kojic acid market will reach 39 million USD [7].

Psoriasis is an auto-immune chronic inflammatory skin disorder characterized by hyperproliferation of keratinocytes and the formation of abnormal hyperkeratotic plaques as the key immunopathological

features. Psoriasis affects 0.27–11.4% of the world population causing detrimental psychological and socioemotional consequences [8, 9]. It is mainly characterized by topical erythema, scaling and increased epidermal thickness. It may result in low-grade systemic inflammation. Psoriasis may cause an increase in spleen weight and cell numbers [10]. It increases the number of T cells, CD + 4 and CD + 8. Psoriasis pathogenesis is not fully understood. However, it has already been proved that psoriasis results from triggers such as trauma, stress, infections and chemicals that stimulate the overexpression of cytokines, most probably the interleukins (IL23/IL17) axis [11]. Overexpression of these cytokines in addition to others such as IL22 and TNFα contributes to inflammation and keratinocytes proliferation [12].

With the absence of definitive treatment and new therapies, repurposing already known and approved drugs represents a smart, safe, and cost-and time-saving approach for the discovery of new anti-psoriatic molecules with reduced risk of failure in clinical trials [13].

The inflammatory nature of this disease, the hyperproliferation of keratinocytes and the functional symbiosis between keratinocytes and melanocytes inspire the search for anti-inflammatory and anti-melanoma agents as potential anti-psoriatic molecules. Of its anti-inflammatory, antiproliferative and anti-melanoma attributes, kojic acid represents an attractive candidate for anti-psoriatic research [14–18]. However, kojic acid suffers from stability issues being sensitive to oxidation, heat and light which necessitate the development of suitable delivery systems for kojic acid to tackle these physicochemical limitations [19].

Nanoencapsulation is considered a good approach to overcome the limitations associated with the conventional administration of several therapeutic agents [20]. Several nanocarriers have been developed to improve skin penetration of topically applied drugs such as liposomes, ethosomes, niosomes, transferosomes, and bilosomes that have shown promising results in dermal drug delivery [21, 22]. Among these carriers are spanlastics which are novel nano vesicular, elastic, surfactant-based drug delivery systems consisting mainly of span and edge activators, that may increase the aqueous solubility, improve formulation flexibility and regulate drug release [23]. Spanlastics can overcome many limitations of the early-developed niosomes and are suggested as a promising candidate for skin delivery [24, 25].

This work aims to isolate kojic acid from the endophytic fungus *A. oryzae N12* associated with the ornamental plant *Tecomaria capensis* and encapsulate the isolated kojic acid in spanlastics by using a combination of Span 60, Birj 35 and Cremophor rh 40 to avoid toxicity. After *in vitro* characterization, the best formulation was selected to be used in further *in vivo* studies and assess their efficacy in the treatment of psoriasis in the imiquimod-induced psoriasis model in mice. Additionally, the molecular mechanism is approached through *in silico* investigation of kojic acid docking in several anti-psoriatic drug targets. To our knowledge, this is the first report for the preparation and repurposing of kojic acid-loaded spanlastics for imiquimod-induced psoriasis management.

2. Materials

Span 60 was purchased from El Nasr Chemicals Co. Egypt. Spectra por semi-permeable membrane (20KD cut off, Thermo scientific, international equipment trading IET, USA). Tween 80, ethyl alcohol and Birj35 were purchased from El Gomhoria Chemical Co. Cremophor rh 40 was obtained as a gift from Pharco Pharmaceutical Company, Egypt. Vaselin Lanette cream, Fagron, and Imiquimod (ALDARA® cream 5%) were purchased from MEDA Pharmaceuticals, Germany. Hematoxylin and Eosin were obtained from (Sigma Aldrich, USA). All other chemicals were of analytical grade.

3. Methods

3.1. Enhanced production of Kojic acid from *Aspergillus oryzae* N12

3.1.1. Fungal isolation and identification

From the stems of *Tecomaria capensis* (Thunb.) Lindl. (Bignoniaceae), collected from El-Orman Garden, Giza, Egypt in 2019, a new fungal isolate *Aspergillus oryzae N12* was obtained and characterized based on morphological and ITS sequencing data. The procedure was a continuation of our ongoing effort to isolate bioactive compounds from plant-associated endophytes. Voucher specimens were kept in the fungarium of the Department of Pharmacognosy, Faculty of Pharmacy, Ain Shams University under the code of PHG-F-AO-449 [26, 27].

The sequencing region covered included the region starting from ITS1 and spanning the regions 5.8SrRNA, and 28S rRNA to the ITS4 in the isolated fungal strain. Bioedit software was utilized to create the consensus sequences, which were further matched to the published sequences in the National Center for Biotechnology Information (NCBI). The isolated strain TC_N12 matched with the highest similarity to *Aspergillus oryzae* strain NG203 with 99% identity and query coverage. The gene sequence was registered in the World Data Centre for Microorganisms (Wdcm) with a registration identifier FN 571634.

Potato dextrose agar (PDA), with and without antibiotic addition, was used to grow and purify the fungal strain. Large-scale culture was carried out in 3 (1 L Erlenmeyer flasks) for 21 days on rice media prepared with a recipe of (100 g of rice in 110 mL of distilled + 0.01 malt extract) and autoclaved. The culture was kept in static condition for three weeks at 25°C. After sporulation and consumption of media, 4 L ethyl acetate was used to extract the whole culture, and 250 mL was added to each Erlenmeyer flask successively, to yield a final dry weight of 5.3 g [27].

The extract was evaporated to dryness using a rotavap before partitioning between 90% MeOH-H_2O and n-hexane. The polar fraction was combined and subjected to a silica gel 60 column chromatography using solvent system DCM: MeOH of increasing polarity (10% – 100%). The fractions eluted between 80% and 60% methanol revealed a heavy precipitate of white crystals of 11.5 g, which was purified and identified by NMR 1D spectroscopic techniques [28].

3.1.2. ^{1}H NMR and ^{13}C NMR of kojic acid (5-hydroxy-2-hydroxymethyl-4H-pyran-4-one)

White crystals, ^{1}H NMR (500 MHz, CD_3OD ppm): 4.41(2H, s, CH_2O), 6.50(1H, s, H-3), 7.93(1H, s, H-6). ^{13}C NMR (125 MHz, CD_3OD ppm): 59.8(C-1), 109.4(C-3), 139.5(C-6), 145.8(C-5), 169.1(C-2), 175.2(C-4) See reference [28].

3.2. Receptor grid generation and ligand preparation

The crystal structures of five proteins were selected from the protein data bank (www.rcsb.org) to carry out the docking procedures for kojic acid, namely, IL-17A (interleukin-17A) (Pdb ID: 5HI4) co-crystallized with 63P, S1PR (Sphingosine 1-Phosphate Receptor (Pdb ID: 3v2W) co-crystallized with ML5phosphonic acid, cathepsin S (Pdb ID: 5QC5) co-crystallized with BAJ, and PDE-4 (Pdb ID: 5K1I) co-crystallized with 6PT. the enzymes crystal structures were prepared by removing water molecules and other trivial small molecules. The protein preparation module was employed for each of these crystal structures to produce the optimized and minimized protein-ligand complexes, which are separated and saved. The native ligands were utilized to locate the grooves where the binding interactions will take place using the Maestro Glide Xtra precision protocol after generating adequate grids with the Receptor Grid Generation tool. Both the native ligands and kojic acid were prepared using the Ligprep tool where they were energy minimized in 2500 iterations by employing the OPLS 2005 forcefield, adding hydrogen to produce accurate 2D structures [29].

3.3. Molecular docking

The Glide XP tool was employed to calculate, based on extra precision criteria, the binding affinity of each of the ligands and kojic acid to the receptor. The XP score was extensively calculated based on the pose ranks, afforded by the XP scores following the equation:

Docking score (Glide score) = a*vdW + b*Coul + Hbond + Lipo + Metal + RotB + site

In the case of having equal pose ranks, the E-model property was utilized for selection since it provided a more accurate estimation of binding for conformers based on different weights of Van der Waals and electrostatic force field components. In the receptor grid generation, standard grid box dimensions were assigned as 13 Å × 13 Å × 13 Å with a Van der Waals factor of 1 and 0.25 workload control factor, which was sufficient to enclose the size of selected ligands. Validation of the docking systems was conducted by re-docking the co-crystallized ligands after saving them in separate files and carrying out superposition procedures to measure the RMSD values revealed to be 2.335 for 3V2W, 2.0471 for 5QC5, 0.0038 for 5K1I, 0.0014 for 5HI4, and 0.0240 for 2YDO (Fig. 2).

3.4. Development of Kojic acid-loaded spanlastics formulations

Kolic acid spanlastic dispersions were prepared using the Ethanol injection method as first described by Kakkar and Kaur [23]. Kojic acid and span 60 were dissolved in ethanol. In another beaker edge activator (s) were dissolved in a calculated volume of distilled water. The ratio of the organic phase to the aqueous phase was 1: 5 v/v. The weight ratio of span: edge activator (s) is illustrated in Table 1. Span ethanolic solution was added dropwise to the aqueous phase while the last was stirred on the magnetic stirrer (Wisestir, MSH20A, PMI Lab instrument, UK).

Table 1
Composition of spanlastics formulations

Formula	Kojic acid	Edge activators (EA)		Water	Span 60	Ethanol	Span: EA(S)	Solvent
		Birj 35	Cremophor rh 40					
F1	-	-	100 mg	8.3 ml	100 mg	1.7 ml	50: 50	10 ml
F2	-	50 mg	50 mg				50: 25: 25	
F3	10 mg	-	100 mg				50: 50	
F4	10 mg	50 mg	50 mg				50: 25: 25	

Stirring was continued to evaporate ethanol until obtaining our final spanlastic dispersion loaded with the calculated dose of Kojic acid [30]. Then, a water bath sonicator (POWER Sonic 405, USA) was used for 5 min to optimize the particle size of the produced dispersions [31].

3.4.1. In vitro characterization of spanlastics

3.4.1.1. Particle size, zeta potential & Poly Dispersity Index

The average Particle size, zeta potential and polydispersity index (PDI) of the prepared spanlastic dispersions were determined using Zeta sizer Nano ZS (Malvern Instruments, Malvern, UK). Samples of each formulation were diluted using distilled water to obtain a final concentration of 0.01 wt. % to avoid aggregation of particles [32].

Zeta potential values of the systems were determined according to the electrophoretic light scattering technology using a Laser Doppler Anemometer coupled with the previously used zeta sizer (Malvern Instruments, Malvern, UK). The technique analyzes the electrophoretic mobility of vesicles under an electric field [33]. All measurements were performed in triplicates.

3.4.1.2. Entrapment Efficiency (EE) %

A portion from each formulation containing 1 mg of kojic acid was centrifugated using a cooling centrifuge (Pro Research K2015 R, Centurion Scientific Ltd, UK) at 15000 rpm for 1 h at 4°C and the

supernatant was separated. The sediment was rewashed with distilled water and vortexed (vortex mixer, Bionex) and the aforementioned procedure was repeated for the resulting dispersion.

The second supernatant was separated in another test tube. The unentrapped Kojic acid was calculated by determining the drug content in the two separated supernatants (1, 2) by spectrophotometric measurement at λ max = 268 nm using UV/vis spectrophotometer (Jenway 6305 single beam spectrophotometer) [34]. The sum of drug content in both supernatants represents the un-entrapped drug. The entrapped drug percentage is calculated as follows:

$$\%EE\,(indirect) = \frac{Totalkojicacidamount - amountofunencapsulatedkojicacid}{TotalKojicacidconcentration}\text{x}100$$

3.4.1.3. *In vitro* drug release

Samples containing 2 mg drug were added to a dialysis bag (20KD cut off, SpectraPore, Thermo Scientific, IET, USA), the bags were properly sealed and incubated in 200 ml phosphate buffer pH 7.4 to ensure sink conditions [35]. A paddle-type dissolution tester (RC-6, Nanbei, China) was used, rotating at 50 rpm with temperature adjusted to 32 ± 0.5°C [25]. At predetermined sampling points, a 5 ml medium sample was withdrawn at predetermined intervals and immediately replaced with another 5 ml of equally warmed buffer. The percentage of kojic acid released was determined using UV spectrophotometry at 268 nm [34]. The experiment was conducted in triplicates.

3.4.1.4. Morphologic examination

Morphological examination was carried out for the selected formulations using a transmission electron microscope (TEM, JEM 1400 PLUS -JEOL, Japan). Samples were prepared by the addition of one drop of spanlastics dispersion after appropriate dilution to a 300-mesh carbon-coated copper grid. Then, the drop was allowed to settle for 5 min to adhere to the carbon substrate to ensure its dryness. After that, the samples were investigated using TEM.

3.5. *In vivo* evaluation of selected modified spanlastics

3.5.1. Animals

Adult male Swiss albino mice (18–25 g) were obtained from the animal facility of the National Research Center, Cairo, Egypt. Animals were allowed to acclimate for at least 1 week before the experiment started. The mice (5–6 per cage) were housed in a conditioned atmosphere at a temperature of 22 ± 3°C and humidity of 50–55% with a 12h light/ dark cycle and free access to food and water. The study complied with the Guide for the Care and Use of Laboratory Animals published by the US National Institutes of Health (NIH Publication No. 85 – 23, revised 2011) and was approved by the Ethics Committee for Animal Experimentation of the Faculty of Pharmacy, Ain Shams University (REC 226). All efforts were made to minimize animal discomfort and suffering.

3.5.2. Study design

Thirty-six mice were randomly allocated into six groups (n = 5–6). All mice had their backs shaved. The study duration was full 7 days from the start of the first application. The *in vivo* experimental protocol is illustrated in Fig. 3. In group 1 (negative control/Vaseline), the vehicle cream (Vaseline Lanette cream, Fagron) was applied to the shaved back. Group 2 (positive control): psoriasis was induced in mice by applying Imiquimod cream (ALDARA® cream 5%) daily at a dose of 62.5 mg on the shaved back and in the right ear of mice. Group 3, Group 4 and Group 5 received the same dose of Imiquimod cream (ALDARA® cream 5%) as Group 3, however, group 4 and Group 5 were treated daily with plain spanlastic formulation and F4, respectively. The concentration was 0.1% w/w [36]. All groups were examined for erythema and scaling at days 0, 2, 4 and 7. On day 7, animals were anaesthetized using thiopental sodium (50 mg/kg i.p.), then sacrificed by cervical dislocation. Splenomegaly of mice was assessed. The shaved area of skin on their backs was immediately excised. A 4 mm punch biopsy of lesional skin was fixed in formalin and paraffin-embedded for histological analysis. The remaining lesional skin was snap-frozen in liquid nitrogen and stored at − 80°C [37] to be further used in PCR tests for measuring gene expression of pro-inflammatory cytokines.

3.5.3. Visual examinations

3.5.3.1. Erythema & scaling

To score the severity of psoriasis, Erythema and scaling were scored according to a predetermined schedule. The scoring system was based on the clinical psoriasis area and severity index (PASI) [38]. Erythema and scaling scores started from 0 which is none, 1 which is mild, 2 as moderate, 3 considered severe and 4 which is very severe. Scoring for each group was carried out on days 0, 2, 4, and 7. The results were recorded as evidence of psoriasis progress or amelioration.

3.5.3.2. Splenomegaly

Animals were weighed on day 0 and day 7. After the animals were euthanized and the skin was excised, we extracted the spleen of one animal per group. the spleen was weighed using an electric balance (Cubis®, Sartorius lab instrument, Germany). The percentage weight of the spleen from the total animal weight was determined. We compared the spleen weight % of groups 3, 4 and 5 to the other three control groups to investigate the effect of treatment on spleen weight [10].

3.5.3.3. Histopathology

Skin tissue samples were flushed and fixed in 10% neutral buffered formalin for 72 h. Samples were trimmed and processed in serial grades of alcohols, cleared in Xylene, and samples were infiltrated and embedded into the Paraplast tissue embedding media. 4µm thick tissue sections were cut by rotatory microtome for demonstration of skin layers in different samples.

Tissue sections were stained with Hematoxylin and Eosin as a general morphological examination staining method and then examined by using a light microscope. All standard procedures for sample fixation and staining according to Culling, C.F.A. 2013 [39].

3.5.3.4. Morphometric analysis

Six non-overlapping epidermal fields were randomly selected and scanned from each sample for the determination of epidermal layer thickness. All light microscopic examination and data were obtained by using the Leica Application module for tissue section analysis attached to the full HD microscopic imaging system (Leica Microsystems GmbH, Germany).

3.5.3.5. Quantitative Real-Time PCR (qRT – PCR) IL17A, IL 22 and IL-23

Total mRNA was extracted with Trizol (Invitrogen) and cDNA was synthesized by reverse transcription using an iScript cDNA synthesis Kit (Bio-Red). The qRT-PCR was performed using iQ SYBR Green Supermix (Bio-Red) according to the manufacturer's instructions. The following primers were used to analyze target mRNA expression IL-17A: 5'-CCGACAGAAGCAGGAGATG – 3' (forward) and 5'CTCAGCCCAACCCAAGATAG3'(reverse); IL22:5'GCACCTCTGACACCGTCTAC–3'(forward) and 5'-GCGGTTTGATGGTAGTGTGC-3'(reverse), IL-23:5'- GGTGTCACGGAGGAATCACA3'(forward) and 5'GCATGAGGTTCCGAAAAGCC-3' (reverse).

3.6. Statistical analysis

Data was expressed as the mean ± Standard Deviation (SD). Differences between groups were analyzed using One-way analysis of variance (ANOVA) using Prism 7 software. Statistical differences yielding $P < 0.05$ were considered significant.

4. Results & Discussion

4.1. In silico molecular docking study

The enzymes were selected based on their role in psoriasis metabolic events. Sphingosine-1-phosphate (S1P) (Pdb ID:3V2W) are bioactive lipids with a potential role in ameliorating the immune response and thus autoimmune diseases such as psoriasis as well as other inflammatory factors [40].

Kojic acid binding was compared to the native ligand ML5 and revealed the formation of four hydrogen bonds to Tyr29 at a distance of (1.87), Ala293(2.21), Leu290(2.19) Lys34(2.27); moreover, Pi-cation interaction was noted between Lys34 and the gamma-lactone ring of kojic acid, which reported Glide XP score of -5.178 Kcal/mol compared to the ML5 of Glide XP score of -12.15 Kcal/mol. The lower score was considerably due to the lower number of hydrogen bonds in kojic acid, shorter bond distances and more contacts to the nonpolar residues Val194(1.68) and the polar residues Asn101(1.75), and Glu121(1.90). The negative binding free energy of kojic acid indicated the favorable binding to the core amino acid of the active site, which is Tyr29. Cathepsin S (Pdb ID: 5QC5) is an activating protease involved in the N-terminal truncation of IL-36γ, which regulates inflammation in the skin tissues as in psoriasis. Cathepsin S is a potent target in psoriasis treatment as it is upregulated during the inflammatory cascade of

psoriasis; therefore, its inhibitors are effective drugs for psoriasis [41]. The *in-silico* approach of docking kojic acid in the enzymatic groove of cathepsin S manifested Pi-pi stacking intersection with Phe70 at a distance of 5.45A° conferring a Gibbs free energy value of -4.474 Kcal/mol compared to the native ligand BAJ, which scored better due to more hydrogen bond formation and Pi-cation interaction to the same amino acid Phe70. The combined activity of kojic acid in more than one enzymatic active site together with the *in vitro* and *in vivo* results prepared kojic acid as an anti-psoriatic drug.

Interleukin-17 (Pdb ID: 5HI4) contributes to the comorbidity of psoriasis, particularly the cardiovascular, and other inflammatory disorders by increasing the hyperproliferation of keratinocytes and T-cell mediated inflammation. Down-regulation of IL-17 is an effective approach towards a better prognosis of immunopathogenesis of psoriasis. Many reports indicated the promising aspects of using selective inhibitors for IL-17A rather than traditional biological treatments [42]. In the enzymatic groove of 5HI4, kojic acid effectively occupied the space in the same orientation as the native ligand with a Pi-pi stacking to Phe372(4.33) and two ionic interactions with Gln369(2.19) and Asn321(1.67). Whereas the 6PT XP score was − 7.781Kcal/mol, kojic acid was − 6.057 Kcal/mol clearly due to the closer distance between Phe372 pi stacking and the pyridazine-one ring.

Adenosine receptor (Pdb ID:2YDO) expression is involved in regulating keratinocyte proliferation observed in cases of psoriasis, which is caused and directed by several inflammatory cytokines, which reduce A2B and enhance A2A.agonists and antagonists of A2B or A2A receptors under realistic physiological conditions could play a significant role in the management of psoriasis [43]. For instance, A2A agonists were promising and beneficial to curb epidermal hyperplasia due to 12-O-tetradecanoylphorbol- 13-acetate (TPA) treatment [44]. The molecular docking of kojic acid as well as the native ligand “adenosine” in the binding site of A2A receptor revealed the vital role of Phe168 and Asn253. A hydrogen bond was formed between the carbonyl group of the kojic acid lactone ring and Asn253 at a distance of 1.89A, which rewarded the fitting stability of the compound to be -7.196 Kcal/mol. Pi-pi stacking interaction between the kojic gamma-lactone ring and Phe168 was observed to occur at a closer distance than the native adenosine; however, the more negative Glide XP score of adenosine − 12.641Kcal/mol was probably caused by the extra ionic interactions encountered by AND to Ser277 and His278 within a bioactive physiological distance of 1.99 and 2.12, respectively. It is worth mentioning that the kojic acid hydroxylated lactone ring was powerful enough to bind the core amino acids in all of the five *in silico* investigated enzymes, representing a promising molecular lead structure for further medicinal chemistry modifications to add more groups, mostly polar with a hydrophobic linker, to further impart energetic stability.

Herein the binding of kojic acid was assessed in the PDE-4 binding pocket where it scored a binding score of -6.057Kcal/mol compared to the native ligand 6PT with a score of -7.781 Kcal/mol. Phosphodiesterase plays a vital role in psoriasis where it degrades cAMP to AMP to produce proinflammatory signaling mediators. Currently, some PDE-4 inhibitors are available and approved for use by the FDA such as apremilast and crisaborole, yet their side effects are pronounced [45]. The pi-pi-stacking feature was again important in the 5KI4 groove but the native 6PT was at a closer distance than

kojic acid to Phe372, which accounts for its marginally higher binding score. Both of them interacted with Gln369 and only kojic acid formed another extra hydrogen bond with Asn321, which was of little effect to improve its stability. This analysis rationalizes the significance of adding another hydrophobic ring to kojic acid in an attempt to improve its bioactivity.

4.2. Development of Kojic acid-loaded spanlastic formulations

The choice of spanlastics for nanoencapsulation of kojic acid was attributed to their elasticity, high penetration and efficient drug loading. High elasticity is attributed use of edge activators (EAs) which provide flexibility to the lipid bilayer membranes of these vesicles [46]. These surfactant molecules destabilize the lipid bilayers and, in turn, increase the deformability of the vesicles [47].

Span 60 is a lipophilic nonionic surfactant of HLB 4.7. Span is the main surfactant used in spanlatics as it is responsible for its composition of well-designed mono and/or multilamellar matrix vesicles [48]. Birj 35 and Cremophor rh40 were used as edge activators to enhance penetration, and efficiency and avoid the use of tween 80 which has been proven to cause sort of anaphylactoid reactions which may lead to undesirable effects on the skin when applied topically [49].

The ethanol injection method is considered an efficient method for the preparation of vesicular elastic nanocarriers [50]. Ethanol can decrease the thickness of vesicles by interpenetrating the hydrocarbon chains, thus reducing their particle size, giving the formula net negative charge (negative zeta potential) that resulted in their steric stabilization and improved their EE.

They were modified from the best two basic formulations selected based on their particle size, zeta potential, EE % and drug release. Birj 35 which is hydrophilic with an HLB of about 15 helped in modifying the HLB of the formulation and increased its solubility in the biological media [51]. cremophor rh40 is a hydrophilic nonionic surfactant with HLB ranging from 14–16. The incorporation of cremophor rh40 in the formulation increased the penetration and flexibility of the vesicles to pass across biological barriers such as stratum corneum in the skin [52]. Formulations containing the three surfactants span 60, birj 35 and cremophor rh40 are structurally more efficient because blending more surfactants optimizes HLB and enhances the formulation structure [53].

4.3. *In vitro* characterization of spanlastics formulations:

4.3.1. Particle size, zeta potential and PDI

The particle size, zeta potential and PDI were measured as shown in Table 2. Four modified formulations showed mean vesicle size ranging from 254.83 nm ± 2 in F3 to 210.1 ± 1.2 nm in F2. The mean vesicle size was inversely proportional to the edge activator concentration in the formulation. This can be explained by the fact that birj 35 and cremophor rh40 are hydrophilic surfactants and this hydrophilicity increased the emulsification effect on the vesicles leading to the production of vesicles with smaller particle size [54].

Table 2
In vitro characteristics of spanlastics in terms of particle size, zeta potential, polydispersity index and EE%

Formula	EE%	Vesicle size (nm)	Zeta potential	PDI
F1	NA	215.3 ± 1.03	-35.5 ± 1.3	0.27 ± 0.012
F2	NA	210.1 ± 1.2	-34.6 ± 1.04	0.36 ± 0.05
F3	85.8 ± 1.34	254.8 ± 2.08	-26.6 ± 0.98	0.45 ± 0.04
F4	87.4 ± 0.98	234.2 ± 1.65	-25.4 ± 1.29	0.332 ± 0.023

Zeta potential is an important indication of stability, where formulations with zeta potential values around ± 30 mV are considered stable due to repulsive forces that prevent particle coalescence and aggregation [21, 55, 56]. All values of the four formulations were negative ranging from − 35.5 ± 1.3 (F1) to − 25.4 ± 1.29 in (F4) as shown in Table 2. The higher the concentration of edge activator (s), the lower the negativity of zeta potential. That may be attributed to the effect of the Edge activator which upon increasing its concentration, covers the surface of vesicles and thus has a shielding effect on the negative charge of the vesicles[47].

The polydispersity index PDI of all formulations ranges between 0.27 (F1) and 0.45 (F3) and this confirms the uniformity of vesicles and their low tendency of aggregation [57–59].

4.3.2. Entrapment Efficiency (EE) %

EE % of the vesicles is very important to determine if the drug concentration will be sufficient to achieve the goal of treatment. In Table 2, EE % of the two drug loaded Formulations (F3 and F4) Using a mixture of surfactants in the same ratio of hydrophilic to lipophilic surfactant concentration in F4 improved its EE compared with F3 that was composed of cremophor rh40, their EE % were 87.4% ± 0.98 and 85.8% ± 1.34, respectively. The HLB value of the formulation is the key factor in this process. At a certain HLB value, the vesicle membranes become more efficient and entrap as much as possible of the drug thus EE % is increased [53].

4.3.3. *In vitro* release

Drug release from Kojic acid loaded Basic spanlastics formulations F3, F4 and kojic acid solution is shown in Fig. 6. F4 and F3 had a slower rate of drug release compared with the kojic acid solution which was nearly 100% released within the first 9 h of the release study. F3 and F4 demonstrated sustained release profiles that extended for 24 h. Both formulations demonstrated a burst effect during the first 30 min of the release study. About 12% and 14% of the loaded drug amount were released from F3 and F4, respectively. The higher burst effect and release rate of F4 compared with F3 may be attributed to the effect of particle size on controlling the amount of the drug released. The smaller the particle size, the higher the surface area exposed to the release medium and consequently higher amounts of the drug are released [60].

Based on the particle size and Zeta potentials of the plain spanlastic selected formulations were further modified new formulations (F3: F4). Results of Particle size, Zeta potentials and

From the aforementioned particle size, zeta potential, EE % and in vitro release results, F4 was selected for further characterization.

4.3.4. Transmission Electron Microscope

Morphological examinations of the two selected modified spanlastics F4 that will undergo further *in vivo* study are graphically illustrated in Fig. 7. The micrographs show the development of nano spherical particles with uniform size and low tendency of aggregation which is matching to the results of particle size and zeta potential measurements.

4.4. *In vivo* study

Psoriasis was induced using an imiquimod-induced mouse model that has been reported as an effective model for psoriasis induction [61–64]. Imiquimod is an imidazoquinoline heterocyclic amine which is available in the market in the form of cream under the Brand Name (ALDARA® cream 5%) [65]. The choice of this model was based on its ability to mimic numerous human plaque-type psoriatic inflammatory features concerning skin thickening, erythema, scaling, parakeratosis, acanthosis and neo-angiogenesis, as well as the inflammatory presence of neutrophils, T cells and dendritic cells [61].

4.4.1. Visual examinations

4.4.1.1. Erythema and scaling

Erythema and scaling are the two major symptoms of psoriasis [38]. Scoring of erythema and scaling was carried out according to the predetermined schedule on days 0, 2, 4, and 7 and based on the clinical Psoriasis area and severity index (PASI) [66]. The scoring of erythema and scaling for all groups throughout the seven days of study is shown in Fig. 9. Day 0 measurement was done before application and treatment, so the result was none for all groups. Day 2 is the third day of application and treatment; Day 4 is the fifth day and Day 7 is measurement after study has ended. Skin inflammation started to be observed on Day 2. It was moderate in group 2 (induced model) and mild in the three groups of treatment. On Day 4, variations started to be observed. Group 5 which was treated with F4 showed obvious amelioration and scored mild erythema and scaling while group 3 which was treated with plain spanlastics gel showed severe scaling and moderate erythema and group 4 which was treated with the aqueous drug solution in gel showed moderate scaling and erythema. Groups 3 and 4 were almost the same as group 2 which is the psoriasis induced model by imiquimod without treatment. On Day 7 after the end of the study, the results were very obvious that group 5 completely recovered in terms of erythema and scaling. The formulation was the most efficient in treatment.

That is along with the *in-vitro* characterization regarding release %, EE % and particle size. That was attributed to the potential of blending surfactants [67]. It contains span which is a lipophilic enhancing structure of vesicles and cremophor rh 40 and birj 35 which are hydrophilic enhancing solubility and drug release. Group 2 which is the psoriasis model showed severe erythema and very severe scaling. Group 4 showed moderate scaling and erythema. That can be summarized as follows, group 5 which was treated by F4 preparation is the group that completely recovered from erythema and scaling, and group 4 which contained drug solution was in the second rank in relieving symptoms. Photos of the animals' shaved backs from all groups are shown in Fig. 8.

4.4.1.2. Splenomegaly

Spleen weight and number of cells can be affected by psoriasis induction [10]. The results of spleen weight percentages are demonstrated in Table 3. In the negative control group

Table 3
Spleen weight percentage for all animal groups

Group Name	Average Spleen Weight (gm)	Average Animal Body Weight (gm)	Average Spleen Weight % From Body Weight
Group1	0.13 ± 0.01	25 ± 1.23	0.52%
Group 2	0.53 ± 0.05	25.5 ± 1.09	2.07% (P < 0.05) *
Group 3	0.34 ± 0.08	24.7 ± 1.06	1.37% (P < 0.05) #*
Group 4	0.29 ± 0.23	26.1 ± 1.7	1.11% (P < 0.05) #*
Group 5	0.24 ± 0.89	24.5 ± 1.56	0.97% (P < 0.05) #
* Statistically significantly different from negative control groups. # Statistically significantly different from the Positive control group.			

(group 1) it can be noted that the spleen weight % is below 0.8%. While Group 2 imiquimod-induced psoriasis, spleen weight % increased to reach 2.07%. On the other hand, in group 5 treated with F4, spleen weight % was nearly normal which is almost 1% of body weight. Group 3 and group 4 demonstrated a slight increase in spleen weight to reach 1.37% and 1.11%, respectively. It can be concluded that the more efficient the treatment that controls psoriasis, the fewer spleen weight changes.

4.4.2. Histopathology

The microscopic examination of different mice skin samples is illustrated in Fig. 10. Results revealed that group 1 demonstrated normal histological structures of skin layers with almost intact thin epidermal stratified squamous epithelium, intact dermal layer with abundant hair follicles and normal organization of collagen fibres with minimal inflammatory cell infiltrates. Also, intact subcutaneous tissue was observed. Group 2 showed the same records as Group 1 samples without records of abnormal alterations of epidermal/dermal structures (Same annotation). Group 3 revealed significant hyperplasia and

increased thickness of the epidermal layer accompanied by occasional intraepithelial lymphocytic infiltrates and moderate sub-epidermal mononuclear inflammatory cells infiltrates with a higher density of dermal collagen bundles. Group 4 showed only a mild decrease of epidermal thickening with the persistence of inflammatory infiltrates as well as a higher density of thick dermal collagen bundles records. Mild to moderate degenerative changes and karyopyknosis in the epidermal basal cell layer were also noted. On the other hand, group 5 showed significant improvement in morphological structures of most samples with almost well-organized, thin epidermal epithelium with few scattered degenerated keratinocytes as well as normal dermal collagen fibres with mild inflammatory cell infiltrates.

4.4.3. Morphometric analysis

Table 4 shows the morphometric analysis of epidermal thickness. The results confirmed the histopathological observations. Group 5 demonstrated almost as healthy and normal epidermal thickness as those of group 1. That is aligned with the visual examinations and confirms the efficiency of treatment with F4. Group 2 showed a significant increase in epidermal thickness due to the induction of psoriasis by imiquimod with no treatment. Group 3 is almost the same as Group 2 and that demonstrates that treatment with plain spanlastics did not make any significant difference in the epidermal thickness. Group 4 did not show a significant difference from group 3 and that confirmed that treatment with drug solution was not efficient in recovering the epidermal thickness.

Table 4
Epidermis Thickness of all animal groups.

Group Name	Epidermal Thickness (µm)
Group1	13.1 ± 2.01
Group 2	85 ± 1.67 (P < 0.05) *
Group 3	65.83 ± 1.89 (P < 0.05) *
Group 4	55.38 ± 1.34 (P < 0.05) * #@
Group 5	16.3 ± 1.12(P < 0.05) #@
Value = mean ± SD	
@ Statistically significantly different from group 3 and group 4re.	
* Statistically significantly different from negative control groups. # Statistically significantly different from the Positive control group.	

4.4.4. Quantitative Real-Time PCR (qRT – PCR) IL17A, IL 22 and IL-23

Recent studies suggested the functional role of IL-23 /IL17A in the pathogenesis of psoriasis [68]. IL-22 can along with Interleukins (IL-23/IL17A) induce many of the pathogenic phenotypes from keratinocytes

and disease progression [69]. Imiquimod (ALDARA® cream 5%) induces the synthesis of proinflammatory cytokines and results in over-gene expression in the interleukins (IL23/IL17A) axis [65]. Figure 11 illustrates that group 2 with the imiquimod psoriasis model had a significant increase in relative mRNA expression levels when compared to the negative control group (group 1). This could be attributed to the inflammatory effect of imiquimod that increases the levels of inflammatory cytokines including IL-17A, IL-22 and IL-23As shown in Fig. 11. Animals treated by Formula F4 (group 5) showed comparable levels of relative mRNA expression levels to the negative control group (group 1). There was no significant difference between F4 treated group and negative control groups in terms of mRNA gene expression of IL-23. These results confirmed the efficient anti-inflammatory action of the F4 formula and its high potential in psoriasis treatment. Relative mRNA gene expression of different interleukins was decreased significantly in animals treated by kojic acid solution (group 4) and free drug blank formula (group 3) when compared to the positive control, however animal group treated by F4 showed the most significant decrease in gene expression when compared to the positive control group ($P < 0.05$).

Gene expression results of this study made a clear explanation of the variations in erythema and scaling scores, splenomegaly, and histopathological and morphometric changes among different groups. Relative mRNA expression of different interleukins was used to measure the efficiency of different drug formulae in the treatment of psoriasis. Induction of psoriasis by imiquimod induced the synthesis of proinflammatory cytokines and resulted in overexpression of the interleukins (IL23/IL17) axis and IL-22 [65]. That was reflected in inflammatory cytokines levels and resulted in inflammatory signs (erythema and scaling) besides the probable systemic inflammation in the form of splenomegaly [10]. Induction of psoriasis by imiquimod also had a direct impact on keratinocyte proliferation and epidermal cell differentiation [38] hence significant histopathological and morphometric changes occurred in the Positive control group when compared to negative control groups.

Kojic acid's role in activating (SirT1) and downregulation of NF-κB resulted in the inhibition of cell differentiation, counteracting the overexpression of some cytokines especially (IL-17 – IL -23 axis) and regulating immune response and inflammations [70]. These effects occurred in different treatment groups but with some variations according to the composition of spanlastics formulae used in treatment. F4 achieved the best results in terms of improvement of Erythema and scaling, recovering normal epidermal thickness and skin morphology, and retaining the normal weight and structure of the spleen. This could be explained by the results of relative mRNA expression of proinflammatory cytokines in the F4 formula which showed the least differences from those of negative control groups. F4 composition of a certain ratio of surfactants (span 60: birj35: cremophor rh40 equal 50: 25: 25) provided it with superior properties in terms of drug solubility, release, penetration and localization in different skin layers. That made the F4 formula superior in the treatment of psoriasis.

5. Conclusion

Spanlastics formulations of Kojic acid with concentrations of 50% span 60, 25% birj 35 and 25% cremophor rh40 were successfully prepared by ethanol injection technique and demonstrated superior

drug entrapment and sustained release profile. The selected formula showed high entrapment efficiency (87.4% ± 0.98) and small mean vesicle size (234.2 ± 1.65 nm). TEM showed spherical vesicles of smooth surface structure. The selected formula also showed superiority in relieving psoriasis symptoms and maintaining healthy skin with the least changes in mRNA expression of inflammatory cytokines. Moreover, the histopathological analysis and splenomegaly examination confirmed its safety profile. The present work successfully represents a new safe efficient biofriendly formulation of kojic acid as an excellent topical alternative delivery system in the treatment of psoriasis with much fewer side effects comparable to systemic treatments.

Declarations

Credit authorship contribution statement

A.Y.M: Experimental, writing original draft, editing, conceptualization, Methodology and software.

Mariam Zewail: Formal analysis, Investigation, writing- original, Visualization, resources and Funding acquisition.

Passent M.E. Gaafar: Validation, Supervision, Writing – original draft, Methodology.

Haidy Abbas: Validation, Writing -review &editing, Methodology, Supervision.

N.I: Conceptualization, writing original draft, methodology.

Declaration of Competing Interest

The authors declare that they have no known competing financial interests or personal relationships that could have appeared to influence the work reported in this paper.

Compliance with ethical standards

All institutional and national guidelines for the care and use of laboratory animals were followed

Funding

This research did not receive any specific grant from funding agencies in the public, commercial, or not-for-profit sectors.

References

1. Moussa, A.Y., et al., *New insights into antimicrobial and antibiofilm effects of edible mushrooms*. Food Research International, 2022: p. 111982.
2. Kemkuignou, B.M., et al., *Terpenoids and meroterpenoids from cultures of two grass-associated species of Amylosporus (Basidiomycota)*. Journal of Natural Products, 2022. 85(4): p. 846–856.

3. AbdelRazek, M.M., et al., *Chemical and Biological Review of Endophytic Fungi Associated with Morus sp. (Moraceae) and In Silico Study of Their Antidiabetic Potential*. Molecules, 2023. 28(4): p. 1718.
4. Amr, K., et al., *Unearthing the fungal endophyte Aspergillus terreus for chemodiversity and medicinal prospects: a comprehensive review*. Fungal Biology and Biotechnology, 2023. 10(1): p. 1–33.
5. Alanzi, A., et al., *Aspergillus co-cultures: A recent insight into their secondary metabolites and microbial interactions*. Archives of Pharmacal Research, 2023: p. 1–26.
6. El-Hawary, S.S., et al., *Natural product diversity from the endophytic fungi of the genus Aspergillus*. RSC advances, 2020. 10(37): p. 22058–22079.
7. de Caldas Felipe, M.T., et al., *Production of kojic acid by Aspergillus species: Trends and applications*. Fungal Biology Reviews, 2023. 45: p. 100313.
8. Magin, P., et al., *The psychological sequelae of psoriasis: results of a qualitative study*. Psychology, health & medicine, 2009. 14(2): p. 150–161.
9. Parisi, R., et al., *National, regional, and worldwide epidemiology of psoriasis: systematic analysis and modelling study*. Bmj, 2020. 369.
10. Frenzel, D.F., et al., *Osteopontin deficiency affects imiquimod-induced psoriasis-like murine skin inflammation and lymphocyte distribution in skin, draining lymph nodes and spleen*. Experimental Dermatology, 2015. 24(4): p. 305–307.
11. Kouris, A., et al., *Proinflammatory cytokine responses in patients with psoriasis*. European cytokine network, 2014. 25(4): p. 63–68.
12. Flutter, B. and F.O. Nestle, *TLRs to cytokines: mechanistic insights from the imiquimod mouse model of psoriasis*. European journal of immunology, 2013. 43(12): p. 3138–3146.
13. Ibezim, A., et al., *A computational multi-targeting approach for drug repositioning for psoriasis treatment*. BMC Complementary Medicine and Therapies, 2021. 21(1): p. 1–8.
14. Yoo, D.S., et al., *A modulatory effect of novel kojic acid derivatives on cancer cell proliferation and macrophage activation*. Die Pharmazie-An International Journal of Pharmaceutical Sciences, 2010. 65(4): p. 261–266.
15. Khan, A., et al., *Antioxidative and Anti-inflammatory Effects of Kojic Acid in Aβ-Induced Mouse Model of Alzheimer's Disease*. Molecular Neurobiology, 2021. 58: p. 5127–5140.
16. Li, T.-X., et al., *Novel kojic acid derivatives with anti-inflammatory effects from Aspergillus versicolor*. Fitoterapia, 2021. 154: p. 105027.
17. Karakaya, G., et al., *Synthesis and cytotoxic evaluation of kojic acid derivatives with inhibitory activity on melanogenesis in human melanoma cells.* Anti-Cancer Agents in Medicinal Chemistry (Formerly Current Medicinal Chemistry-Anti-Cancer Agents), 2018. 18(15): p. 2137–2148.
18. Saeedi, M., M. Eslamifar, and K. Khezri, *Kojic acid applications in cosmetic and pharmaceutical preparations*. Biomedicine & Pharmacotherapy, 2019. 110: p. 582–593.
19. Zilles, J.C., et al., *Biological activities and safety data of kojic acid and its derivatives: A review*. Experimental dermatology, 2022. 31(10): p. 1500–1521.

20. Parveen, S., R. Misra, and S.K. Sahoo, *Nanoparticles: a boon to drug delivery, therapeutics, diagnostics and imaging*. Nanomedicine: Nanotechnology, Biology and Medicine, 2012. 8(2): p. 147–166.
21. Ahmed, S., M.A. Kassem, and S. Sayed, *Bilosomes as Promising Nanovesicular Carriers for Improved Transdermal Delivery: Construction, in vitro Optimization, ex vivo Permeation and in vivo Evaluation*. International Journal of Nanomedicine, 2020. 15: p. 9783.
22. Zewail, M., et al., *Novel Siprulina platensis Bilosomes for Combating UVB Induced Skin Damage*. Pharmaceuticals, 2023. 16(1): p. 36.
23. Kakkar, S. and I.P. Kaur, *Spanlastics—a novel nanovesicular carrier system for ocular delivery*. International journal of pharmaceutics, 2011. 413(1–2): p. 202–210.
24. Arunachalam, A., et al., *Niosomes: a novel drug delivery system*. International journal of novel trends in pharmaceutical sciences, 2012. 2(1): p. 25–31.
25. Maddineni, S., et al., *Dissolution research-A predictive tool for conventional and novel dosage forms*. Asian Journal of Pharmacy and Life Science ISSN, 2012. 2231: p. 4423.
26. Moussa, A.Y., et al., *Caspicaiene: a new kaurene diterpene with anti-tubercular activity from an Aspergillus endophytic isolate in Gleditsia caspia desf*. Natural Product Research, 2021. 35(24): p. 5653–5664.
27. Abdel Razek, M.M., et al., *A New Phenolic Alkaloid from Halocnemum strobilaceum endophytes: antimicrobial, antioxidant and biofilm Inhibitory activities*. Chemistry & Biodiversity, 2020. 17(10): p. e2000496.
28. Ola, A.R., et al., *Single production of kojic acid by Aspergillus flavus and the revision of flufuran*. Molecules, 2019. 24(22): p. 4200.
29. Torky, Z.A., et al., *Chemical profiling, antiviral and antiproliferative activities of the essential oil of Phlomis aurea Decne grown in Egypt*. Food & Function, 2021. 12(10): p. 4630–4643.
30. Rajera, R., et al., *Niosomes: a controlled and novel drug delivery system*. Biological and Pharmaceutical Bulletin, 2011. 34(7): p. 945–953.
31. Essa, E.A., *Effect of formulation and processing variables on the particle size of sorbitan monopalmitate niosomes*. Asian Journal of Pharmaceutics (AJP): Free full text articles from Asian J Pharm, 2014. 4(4).
32. Tantra, R., P. Schulze, and P. Quincey, *Effect of nanoparticle concentration on zeta-potential measurement results and reproducibility*. Particuology, 2010. 8(3): p. 279–285.
33. Bhattacharjee, S., *DLS and zeta potential–what they are and what they are not?* Journal of controlled release, 2016. 235: p. 337–351.
34. Song, L., et al., *Synthesis, antimicrobial, moisture absorption and retention activities of kojic acid-grafted konjac glucomannan oligosaccharides.* Polymers, 2019. 11(12): p. 1979.
35. Marques, M.R., R. Loebenberg, and M. Almukainzi, *Simulated biological fluids with possible application in dissolution testing*. Dissolution Technol, 2011. 18(3): p. 15–28.

36. Negi, P., et al., *Niosome-based hydrogel of resveratrol for topical applications: An effective therapy for pain related disorder (s)*. Biomedicine & Pharmacotherapy, 2017. 88: p. 480–487.
37. Kong, H.H., et al., *Performing skin microbiome research: a method to the madness*. Journal of Investigative Dermatology, 2017. 137(3): p. 561–568.
38. Kjær, T.N., et al., *Resveratrol ameliorates imiquimod-induced psoriasis-like skin inflammation in mice*. PloS one, 2015. 10(5): p. e0126599.
39. Culling, C.F.A., *Handbook of histopathological and histochemical techniques: including museum techniques*. 2013: Butterworth-Heinemann.
40. Liu, L., et al., *Sphingosine-1-Phosphate and its signal modulators alleviate psoriasis-like dermatitis: preclinical and clinical evidence and possible mechanisms*. Frontiers in Immunology, 2021. 12: p. 759276.
41. Ainscough, J.S., et al., *Cathepsin S is the major activator of the psoriasis-associated proinflammatory cytokine IL-36γ.* Proceedings of the national academy of sciences, 2017. 114(13): p. E2748-E2757.
42. Menter, A., et al., *Interleukin-17 and interleukin-23: a narrative review of mechanisms of action in psoriasis and associated comorbidities*. Dermatology and Therapy, 2021. 11: p. 385–400.
43. Andrés, R.M., et al., *Adenosine A2A and A2B receptors differentially modulate keratinocyte proliferation: possible deregulation in psoriatic epidermis*. Journal of Investigative Dermatology, 2017. 137(1): p. 123–131.
44. Arasa, J., et al., *Topical application of the adenosine A2A receptor agonist CGS-21680 prevents phorbol-induced epidermal hyperplasia and inflammation in mice*. Experimental Dermatology, 2014. 23(8): p. 555–560.
45. Milakovic, M. and M.J. Gooderham, *Phosphodiesterase-4 inhibition in psoriasis*. Psoriasis: Targets and Therapy, 2021: p. 21–29.
46. Duangjit, S., et al. *Effect of edge activator on characteristic and in vitro skin permeation of meloxicam loaded in elastic liposomes*. in *Advanced Materials Research*. 2011. Trans Tech Publ.
47. Tayel, S.A., et al., *Duodenum-triggered delivery of pravastatin sodium via enteric surface-coated nanovesicular spanlastic dispersions: development, characterization and pharmacokinetic assessments*. International Journal of Pharmaceutics, 2015. 483(1–2): p. 77–88.
48. Fahmy, A.M., et al., *Penetration enhancer-containing spanlastics (PECSs) for transdermal delivery of haloperidol: in vitro characterization, ex vivo permeation and in vivo biodistribution studies*. Drug delivery, 2018. 25(1): p. 12–22.
49. Coors, E.A., et al., *Polysorbate 80 in medical products and nonimmunologic anaphylactoid reactions*. Annals of Allergy, Asthma & Immunology, 2005. 95(6): p. 593–599.
50. Pando, D., et al., *Formulation of resveratrol entrapped niosomes for topical use*. Colloids and Surfaces B: Biointerfaces, 2015. 128: p. 398–404.
51. Popović-Nikolić, M.R., G.V. Popović, and D.D. Agbaba, *The effect of nonionic surfactant brij 35 on solubility and acid–base equilibria of verapamil*. Journal of Chemical & Engineering Data, 2017.

62(6): p. 1776–1781.

52. Chen, L., et al., *Microemulsion and microporation effects on the genistein permeation across dermatomed human skin*. AAPS PharmSciTech, 2018. 19(8): p. 3481–3489.
53. Weerapol, Y., et al., *Self-nanoemulsifying drug delivery system of nifedipine: impact of hydrophilic–lipophilic balance and molecular structure of mixed surfactants*. AAPS pharmscitech, 2014. 15(2): p. 456–464.
54. Otto, A., J. Du Plessis, and J. Wiechers, *Formulation effects of topical emulsions on transdermal and dermal delivery*. International journal of cosmetic science, 2009. 31(1): p. 1–19.
55. Rahman, H.S., et al., *Zerumbone-loaded nanostructured lipid carriers: preparation, characterization, and antileukemic effect*. International Journal of Nanomedicine, 2013. 8: p. 2769.
56. Zewail, M., et al., *Coated nanostructured lipid carriers targeting the joints–An effective and safe approach for the oral management of rheumatoid arthritis*. Int J Pharm., 2019. 567: p. 118447.
57. Abbas, H. and R. Kamel, *Potential role of resveratrol-loaded elastic sorbitan monostearate nanovesicles for the prevention of UV-induced skin damage*. Journal of Liposome Research, 2020. 30(1): p. 45–53.
58. Abbas, H., N.M. El-Deeb, and M. Zewail, *PLA-coated Imwitor® 900 K-based herbal colloidal carriers as novel candidates for the intra-articular treatment of arthritis.* Pharmaceutical Development and Technology, 2021. 26(6): p. 682–692.
59. Abd-El-Azim, H., et al., *Non-invasive Management of Rheumatoid Arthritis using Hollow Microneedles as a Tool for Transdermal Delivery of Teriflunomide Loaded Solid Lipid Nanoparticles*. International Journal of Pharmaceutics, 2023: p. 123334.
60. Klose, D., et al., *How porosity and size affect the drug release mechanisms from PLGA-based microparticles*. International journal of pharmaceutics, 2006. 314(2): p. 198–206.
61. Jabeen, M., et al., *Advanced characterization of imiquimod-induced psoriasis-like mouse model*. Pharmaceutics, 2020. 12(9): p. 789.
62. Elgewelly, M.A., et al., *Resveratrol-Loaded Vesicular Elastic Nanocarriers Gel in Imiquimod-Induced Psoriasis Treatment: In Vitro and In Vivo Evaluation*. Journal of Pharmaceutical Sciences, 2022. 111(2): p. 417–431.
63. Lin, Y.-K., et al., *Using imiquimod-induced psoriasis-like skin as a model to measure the skin penetration of anti-psoriatic drugs*. PLoS One, 2015. 10(9): p. e0137890.
64. Chen, T., et al., *Involvement of high mobility group box-1 in imiquimod-induced psoriasis-like mice model*. The Journal of Dermatology, 2017. 44(5): p. 573–581.
65. Van Der Fits, L., et al., *Imiquimod-induced psoriasis-like skin inflammation in mice is mediated via the IL-23/IL-17 axis*. The Journal of Immunology, 2009. 182(9): p. 5836–5845.
66. Na Takuathung, M., et al., *Antipsoriatic effects of wannachawee recipe on imiquimod-induced psoriasis-like dermatitis in BALB/c Mice.* Evidence-Based Complementary and Alternative Medicine, 2018. 2018.

67. van den Bergh, B.A., et al., *Elasticity of vesicles assessed by electron spin resonance, electron microscopy and extrusion measurements*. International journal of pharmaceutics, 2001. 217(1–2): p. 13–24.
68. Di Cesare, A., P. Di Meglio, and F.O. Nestle, *The IL-23/Th17 axis in the immunopathogenesis of psoriasis*. Journal of Investigative Dermatology, 2009. 129(6): p. 1339–1350.
69. Ouyang, W., *Distinct roles of IL-22 in human psoriasis and inflammatory bowel disease*. Cytokine & growth factor reviews, 2010. 21(6): p. 435–441.
70. Oliveira, A.L.d.B., et al., *Resveratrol role in autoimmune disease—a mini-review*. Nutrients, 2017. 9(12): p. 1306.

Figures

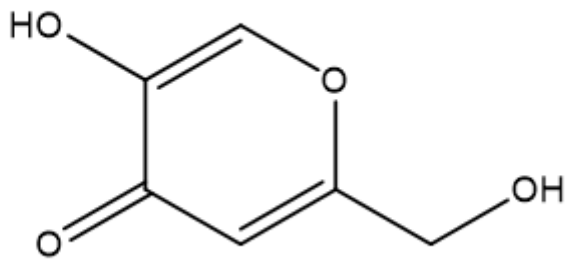

Figure 1

Chemical structure of kojic acid.

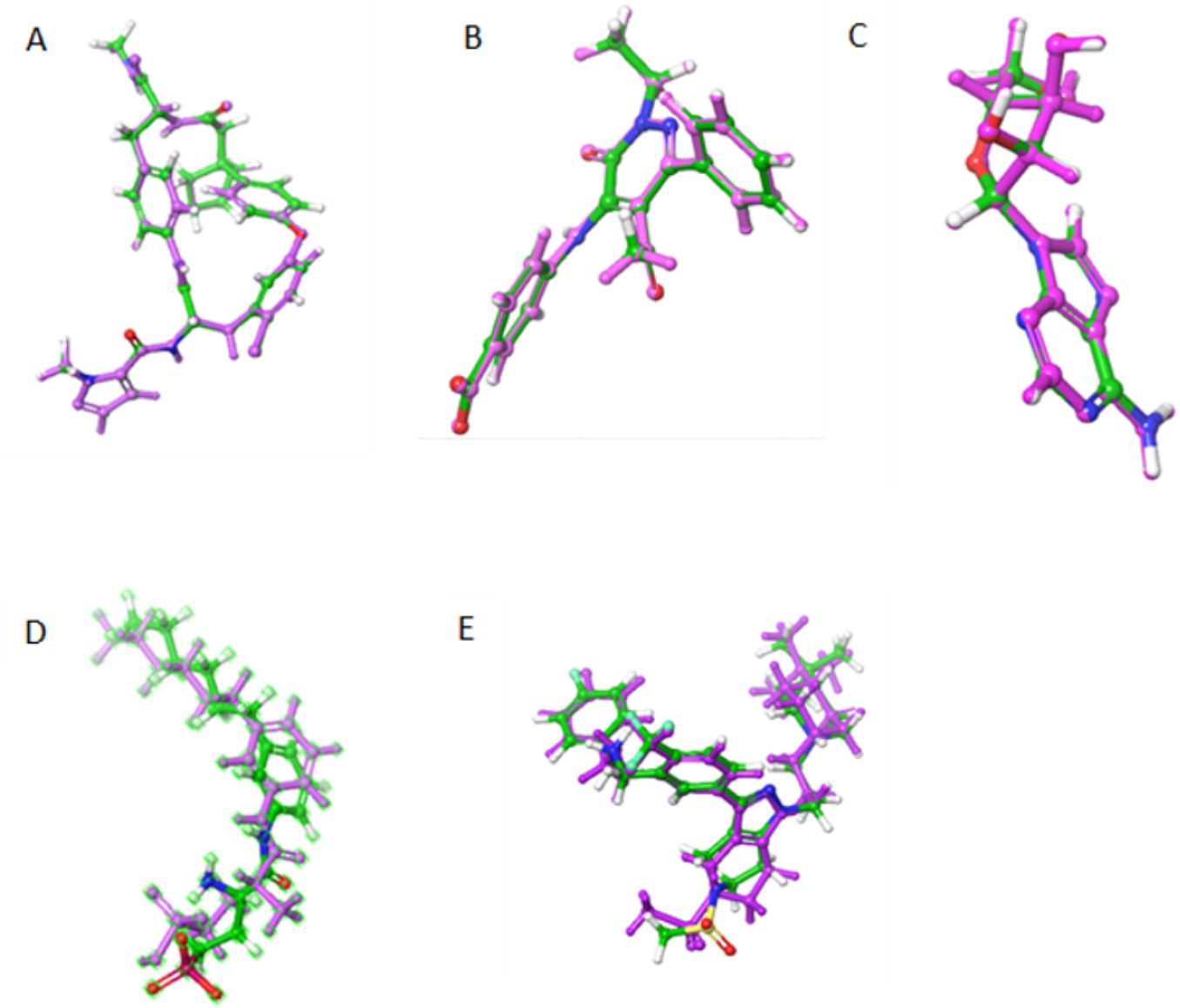

Figure 2

Validation of docking procedures A: 5HI4, B: 5K1I, C: 2YDO, D: 3V2W, and E: 5QC5.

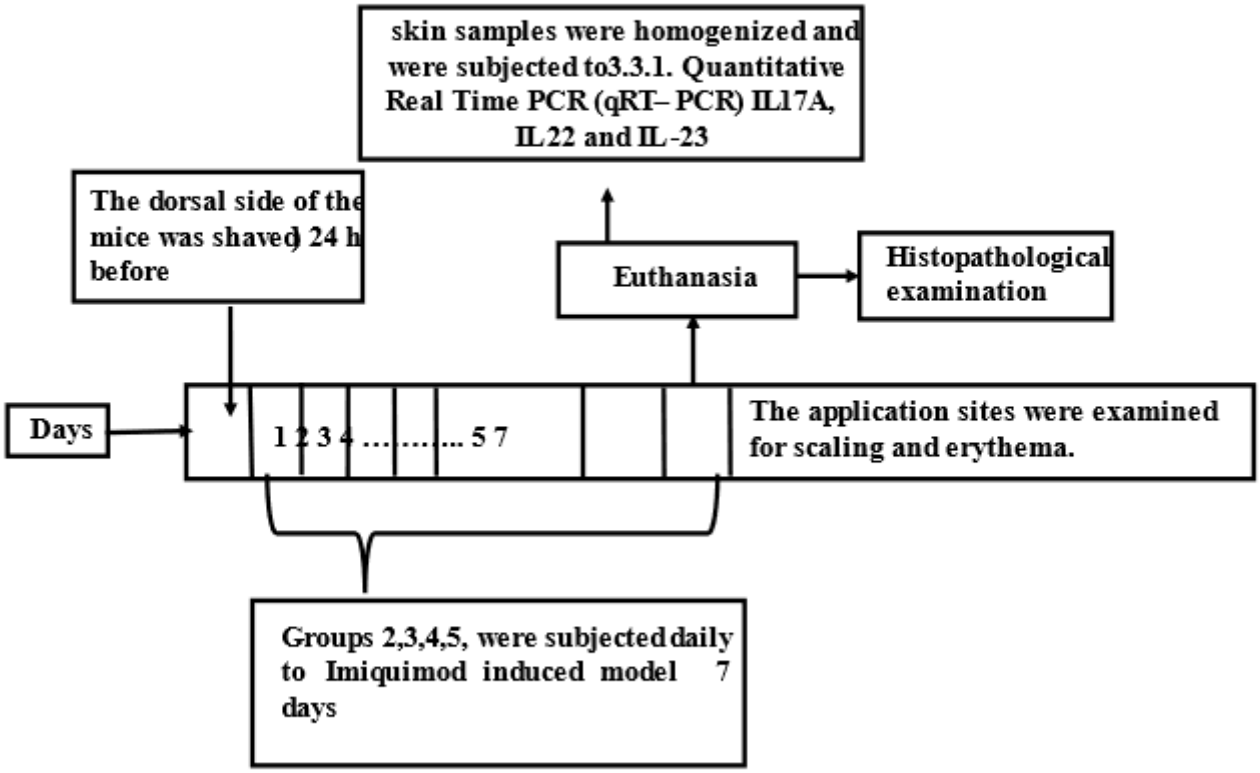

Figure 3

In vivo experimental protocol.

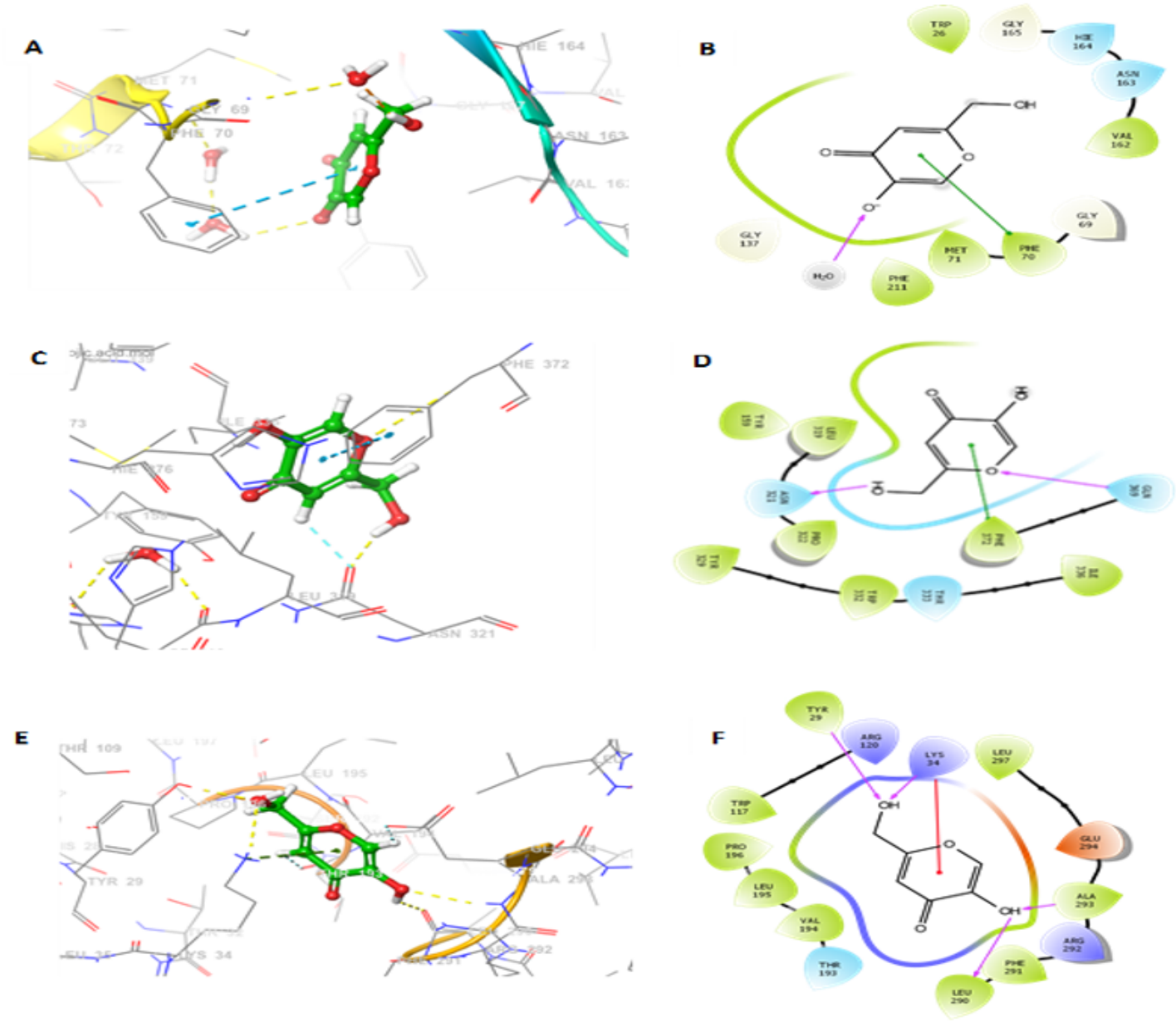

Figure 4

2D and 3D interactions of 5QC5, 5K1I, and 3V2W.

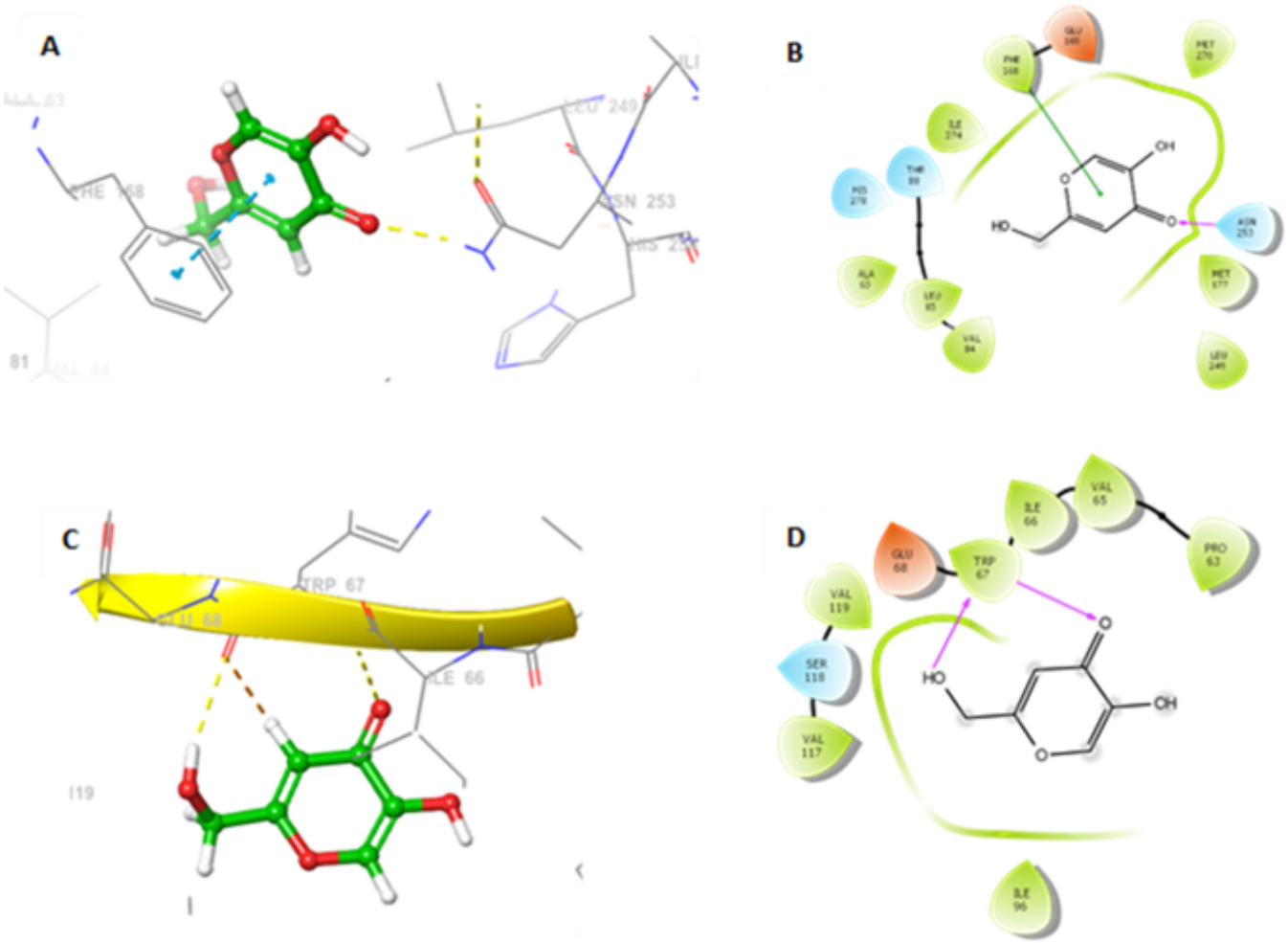

Figure 5

2D and 3D interactions of 2YDO and 5HI4.

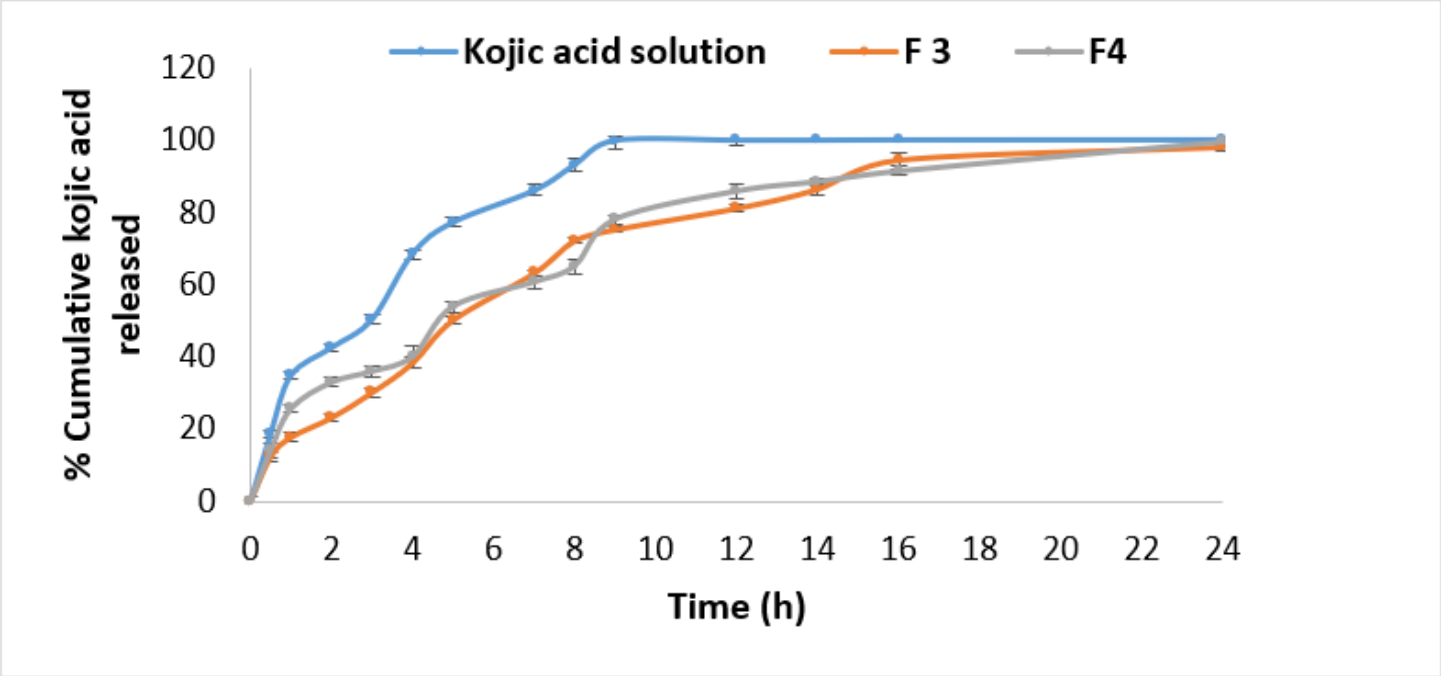

Figure 6

In vitro drug release from spanlastics formulations (F3 and F4) in addition to kojic acid solution. Values calculated as mean ± SD

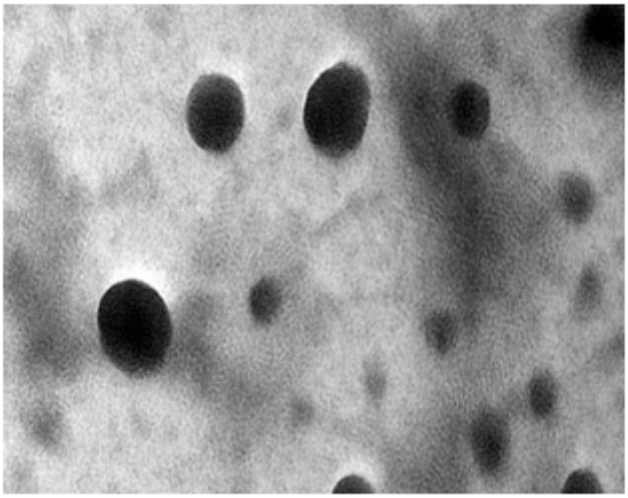

Figure 7

TEM micrograph of selected spanlastics formulation (F4).

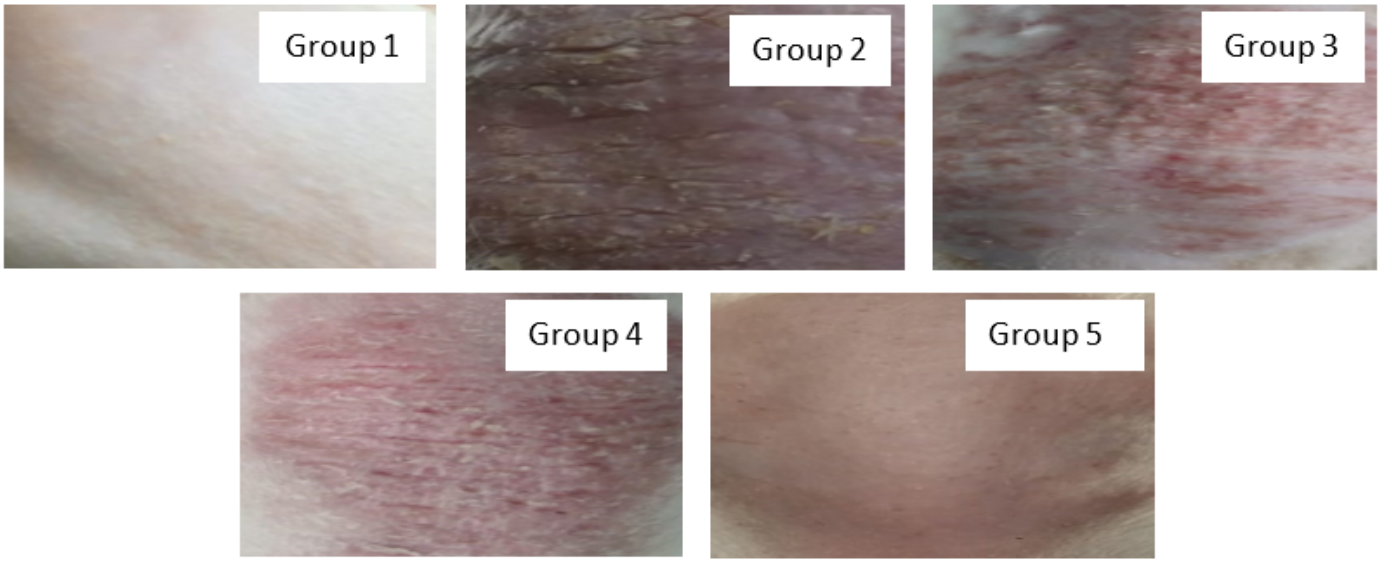

Figure 8

Photographs of the dorsal mice skin after five days of treatment. Group 1 negative control treated only by Vaseline, group 2 Imiquimod induced model without treatment, groups from 3 to 5 are imiquimod induced psoriasis and treated as follows, group 3 plain spanlastics, group 4 kojic acid solution and group 5 by F4.

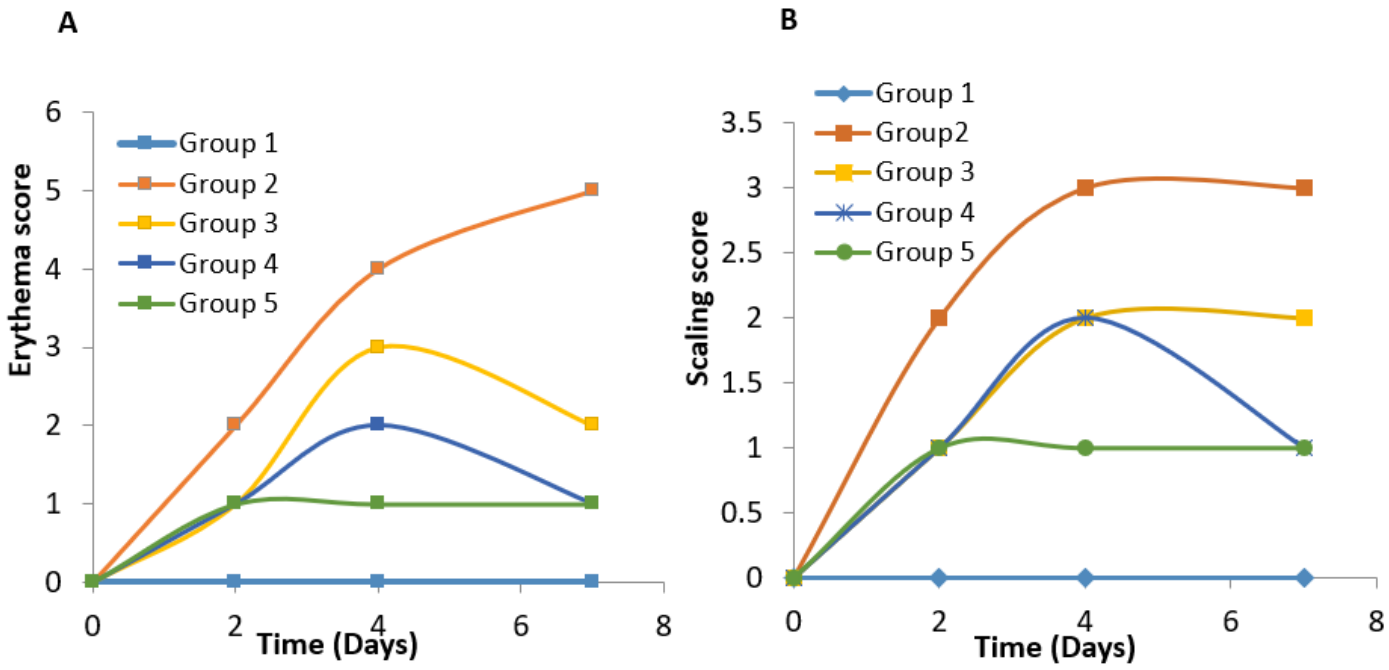

Figure 9

Progress of psoriasis visual signs (A) Erythema (B) scaling.

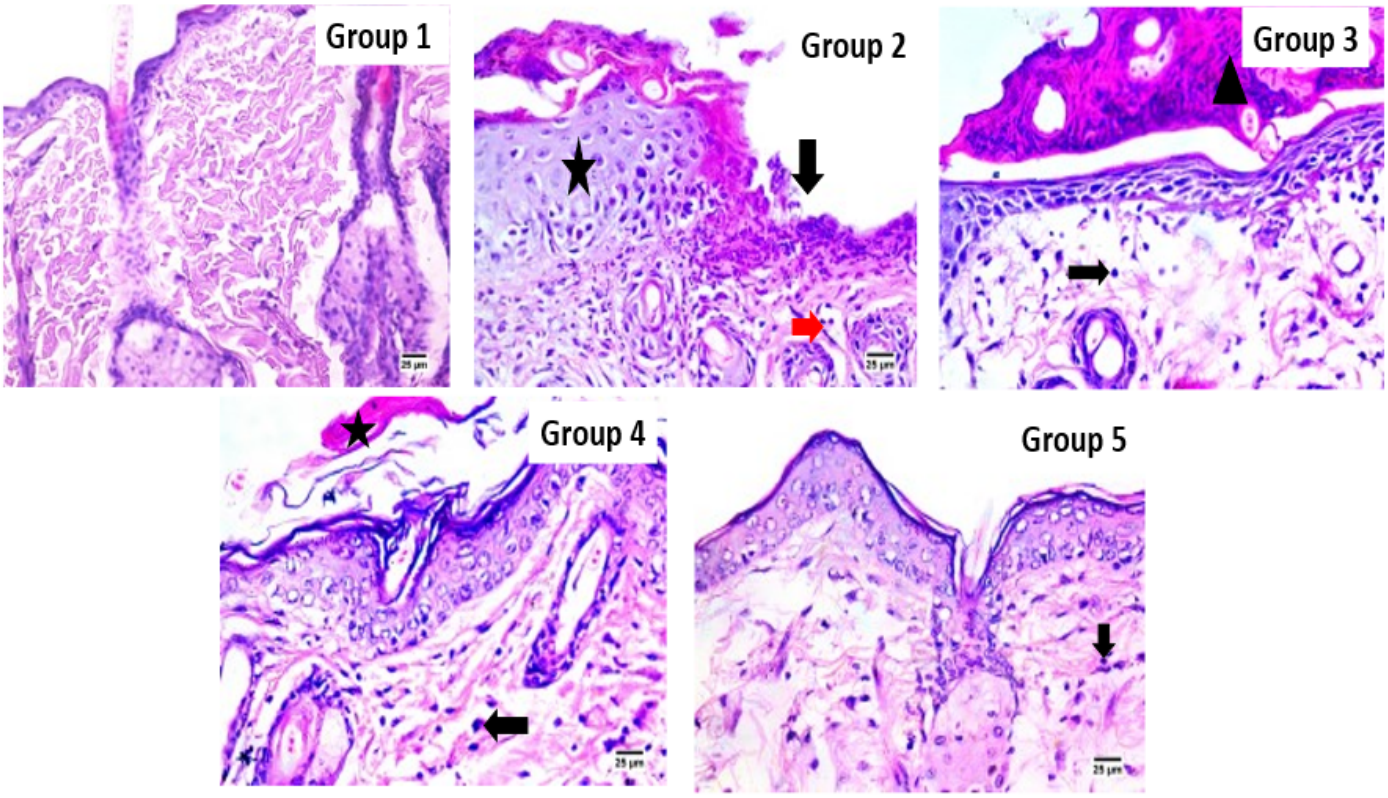

Figure 10

photomicrograph showing group 1 demonstrating normal histological structure of the skin. Group 2 showed ulcer formation covered by serocellular crust (black arrow) with increasing epidermal layer thickness (star) and infiltration of the dermis by mononuclear inflammatory cells (red arrow). Group 3 demonstrated that the epidermal layer was covered by a serocellular crust (star) with infiltration of the dermis by mononuclear inflammatory cells (arrow). Group 4 showed parakeratosis formation (star) with infiltration of the dermis by mononuclear inflammatory cells (arrow). Group 5 infiltration of the dermis by low numbers of mononuclear inflammatory cells (arrow) (Hematoxylin and Eosin stain)

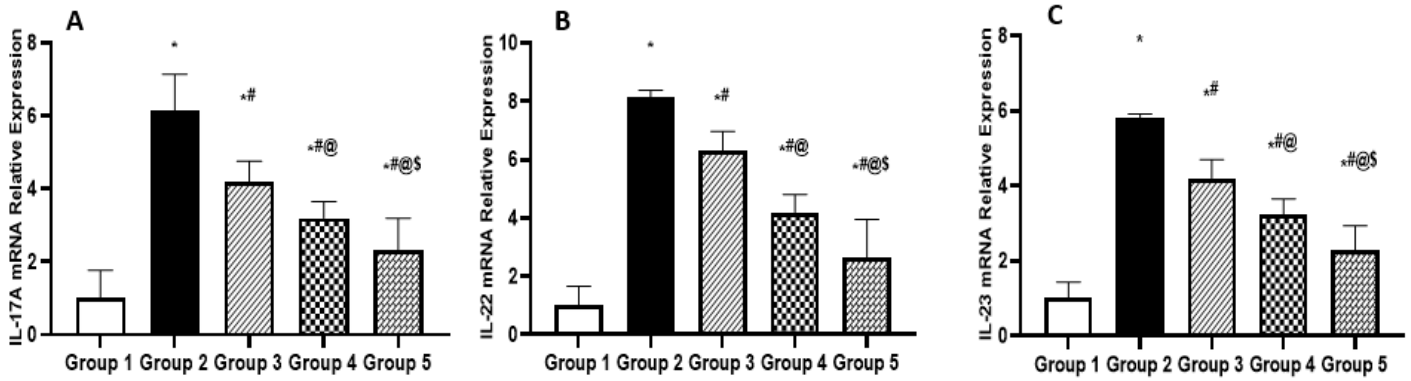

Figure 11

Relative mRNA expression of inflammatory cytokines, (A) IL-17A (B) IL-22 and (C) IL-23 for all animal groups, as an indicator of the anti-inflammatory effect of kojic acid in different formulae. Group (1) negative control treated only by Vaseline, group (2) Imiquimod induced model without treatment, groups from 3 to 5 are imiquimod induced psoriasis and treated as follows, group (3) plain plastic, group (4) kojic acid solution and group (5) by F4. Data presented as Mean ± SD. * statistically significantly different from negative control groups (Group 1) ($P < 0.05$). # statistically significantly different from the positive control group (Group 2) ($P < 0.05$). @ Statistically significantly different from group 3 and $ signicantly different from group 4 ($P < 0.05$).

Supplementary Files

This is a list of supplementary files associated with this preprint. Click to download.

- Graphicalabstract11.pptx